Acknowledgment. This work was conducted under the McDonnell Douglas Research Laboratories (St. Louis) Independent Research and Development Program.

References and Notes

(1) The Imperial Chemical Industries trademark is Victrex PEEK.
(2) Schaefer, J.; Stejskal, E. O. *Top. Carbon-13 NMR Spectrosc.* **1979**, *3*, 284.
(3) Schaefer, J.; Garbow, J. R.; Stejskal, E. O.; Lefelar, J. A. *Macromolecules* **1987**, *20*, 1271.
(4) Torchia, D. A. *J. Magn. Reson.* **1978**, *30*, 613.
(5) Schaefer, J.; Sefcik, M. D.; Stejskal, E. O.; McKay, R. A. *Macromolecules* **1984**, *17*, 1118.
(6) Munowitz, M. G.; Griffin, R. G. *J. Chem. Phys.* **1982**, *76*, 2848.
(7) Burum, D. P.; Linder, M.; Ernst, R. R. *J. Magn. Reson.* **1981**, *44*, 173.
(8) Schaefer, J.; Stejskal, E. O.; McKay, R. A.; Dixon, W. T. *Macromolecules* **1984**, *17*, 1479.
(9) Garbow, J. R.; Schaefer, J. *Macromolecules* **1987**, *20*, 819.
(10) Poliks, M. D.; Schaefer, J. *Macromolecules* **1990**, *23*, 2682.
(11) Clark, J. N.; Jagannathan, R. R.; Herring, F. G. *Polymer* **1988**, *29*, 341.

Registry No. PEEK, 31694-16-3.

Two-Dimensional Solid-State NMR Studies of Ultraslow Chain Motion: Glass Transition in Atactic Poly(propylene) versus Helical Jumps in Isotactic Poly(propylene)

D. Schaefer and H. W. Spiess*

Max-Planck-Institut für Polymerforschung, Postfach 3148, D-6550 Mainz, West Germany

U. W. Suter

Institut für Polymere, ETH Zentrum, CH-8092 Zürich, Switzerland

W. W. Fleming

Almaden Research Center, IBM Research Division, 650 Harry Road, San Jose, California 95120-6099

Received December 5, 1989

ABSTRACT: The deuteron 2D exchange experiment has been applied to study the ultraslow rotational chain dynamics of atactic (aPP) and isotactic poly(propylene) (iPP). The motional mechanism was found to be vastly different for these polymers, reflecting the different chain conformation and packing. Whereas in amorphous aPP in the vicinity of the glass transition a diffusive motion was observed, iPP was shown to perform helical jumps about the helix axis in the crystalline domains at temperatures above 360 K. The temperature variation of the mean correlation times, obtained from an analysis of the aPP spectra based on isotropic rotational diffusion with a distribution of correlation times, follows the WLF equation over 11 orders of magnitude between 10^{-10} and 10 s. The parameters extracted from this fit correspond to textbook values known from macroscopic measurements of the viscoelastic behavior in amorphous polymers. This shows that 2D NMR, although monitoring the chain dynamics via a localized probe, is able to follow the collective dynamics of the glass process. The discrete jump motion observed for iPP is caused by 120° rotations of the 3_1 helix about the helix axis. The relative angle of 113° between the methyl groups before and after the jump is determined from the 2D spectra directly without the need of interfacing a model and agrees with the value calculated from crystallographic data.

Introduction

The macroscopic properties of polymeric materials are often supposed to be governed by the molecular motion of the macromolecular chains.[1,2] The dynamics, in turn, depends on the arrangement of the chains in amorphous or crystalline states. A variety of physicochemical techniques have amply demonstrated the existence of several relaxations in completely amorphous as well as in partially crystalline polymers, and many studies are engaged in elucidating the molecular nature of these relaxations.[1,3,4] Among these techniques pulsed ^2H NMR and ^{13}C NMR have proved to be successful in probing molecular reorientations.[5-8] Most techniques, however, cannot clearly discriminate between different motional mechanisms proposed for polymer chain dynamics. The application of two-dimensional (2D) Fourier transform (FT) methods to the study of molecular motions[9] represents a major step in order to solve this problem: through the 2D exchange experiment the molecular orientation is measured via the NMR frequency *before* and *after* a mixing time t_m during which slow dynamic processes changing the molecular orientation may occur. Therefore, by systematic variation of t_m, the dynamic process can be followed in *real time*. Moreover, the experiment also yields unique geometric information since the angle by which the molecules rotate is measured directly, without the need of interfacing a model.[9,10]

In fact, each 2D exchange NMR spectrum represents a statistically well-defined two-time distribution function.[11] It describes the joint probability density to find molecules with NMR frequencies ω_1 before and ω_2 after the

0024-9297/90/2223-3431$02.50/0

mixing time. For a fixed value of t_m the 2D absorption mode NMR spectrum is an image of the corresponding state of the dynamic process. By variation of t_m the evolution of the motional process can be followed and different motional mechanisms can clearly be discriminated. In ^2H NMR the mixing time may be varied between 10^{-3} s and several seconds, limited by the spin–lattice relaxation.[12] Thus ultraslow motions directly correlated to the mechanical properties become accesible to experiment.

In the present paper we apply this new technique to study the effect of chain configuration, conformation, and packing on ultraslow chain dynamics. Poly(propylene) is an appropriate candidate for this kind of investigation: Stereoregular isotactic poly(propylene) (iPP) forms crystalline regions with well-defined helices melting at 450 K only. In contrast, atactic poly(propylene) (aPP) is amorphous with a glass transition temperature T_g as low as 253 K.

As known from mechanical measurements ultraslow dynamics in the range of 1 Hz to 1 kHz exist in both polymers.[1,4] In iPP the ultraslow motions that occur at elevated temperatures are ascribed to chain motions in the crystalline regions. In aPP such ultraslow motions occur during the glass transition, slightly above T_g. By 2D exchange NMR we can tackle the question of whether the differences in conformation and packing between the stereoregular chains in the crystalline regions on the one hand and the stereoirregular chains in the amorphous state on the other hand reflect themselves in different motional processes. Moreover, in aPP we can try to relate the ultraslow chain motion to the dynamic process associated with the glass transition.

2D Exchange NMR

In order to assist in understanding of the 2D spectra presented below, we give a brief description of the 2D exchange experiment. For details the reader is refered to refs 5, 9, 11, 13, and 14.

Basics. The ^2H NMR spectrum is dominated by the coupling of the electric field gradient with the nuclear electric quadrupole moment. In the case of an axially symmetric field gradient tensor (FGT), as is a good approximation in ^2H NMR, the NMR frequency of the spin $I = 1$ system is given by[15,16]

$$\omega = \omega_0 \pm {}^1/_2\delta(3\cos^2\vartheta - 1) \qquad (1)$$

which depends on the angle ϑ the unique axis of the FGT, i.e., the C–^2H bond direction or the threefold axis of a rotating methyl group, forms with the static magnetic field $\vec{B}_0$, (see below). In eq 1 ω_0 is the Larmor frequency, and $\delta = (3/4)(e_q e_Q/\hbar)$ specifies the strength of the anisotropic quadrupolar interaction. The $\pm$ sign corresponds to the two allowed NMR transitions of the deuteron spin $I = 1$ leading to a symmetric spectrum, centered at ω_0. Thus, in ^2H NMR rotations of polymer chains are monitored through the time-dependent orientations of individual C–^2H bonds or C_3 axes of methyl groups in isotopically labeled samples. For isotropic powders an inhomogeneously broadened line shape (Pake diagram[17]) results with characteristic singularities for $\vartheta = 90°$. In rigid solids $\delta/2\pi$ is ca. 125 kHz for deuterons in C–^2H bonds, and for aliphatic polymer chains $\delta/2\pi$ shows minor variations only. Rapid anisotropic motions on a time scale $\tau \leq \delta^{-1}$ lead to partially averaged tensors. The most prominent example, also pertinent to poly(propylene), is a methyl group rotating about its threefold axis, leading to $\bar{\delta} = {}^1/_3\delta$.[6,8]

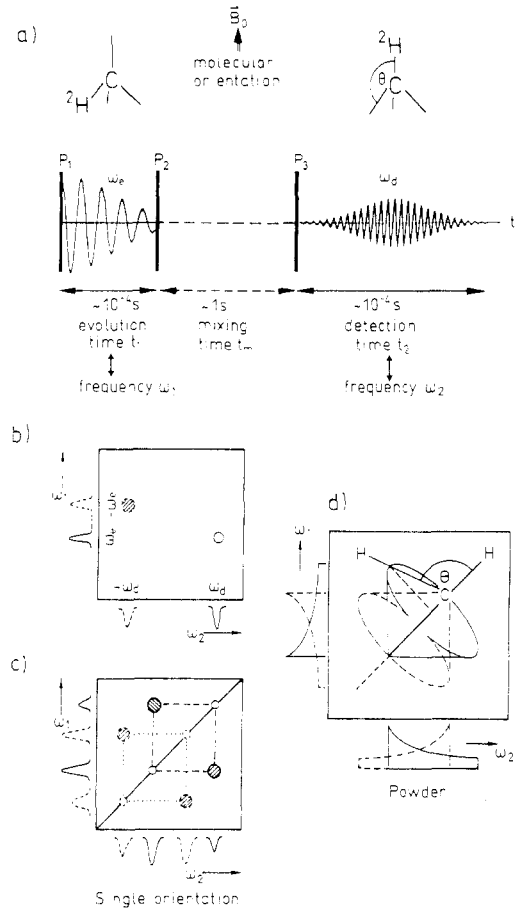

Figure 1. Principle of 2D exchange NMR. (a) Three-pulse sequence. The NMR frequencies ω_e and ω_d correspond to the orientations of the C–^2H bond during the evolution time t_1 and the detection time t_2. (b) A complete exchange of the orientation during the mixing time t_m results in a signal in the 2D exchange spectrum at the position (ω_e, ω_d) and $(-\omega_e, -\omega_d)$. The solid line represents one transition, the dashed line the second transition of the spin $I = 1$ system. (c) Complete ^2H 2D exchange spectrum for the two different orientations given above. If no exchange occurs during t_m, the NMR frequency of a particular C–^2H bond remains the same and only a diagonal spectrum will be detected. If molecular reorientation does occur during t_m, then the frequencies measured in evolution and detection will be different and cross peaks at the intersection of the different frequencies are observed in the 2D plane. The dashed square connects the peaks for one transition, the dotted square the peaks for the second transition. (d) 2D exchange spectrum for a powder sample. All orientations are equally likely to occur, resulting in continuous off-diagonal exchange patterns. In the case of a discrete jump motion about a well-defined angle, the 2D exchange spectrums displays singularities in the form of ellipses, from which the reorientational angle Θ can be determined in a model-independent fashion.

Three-Pulse Sequence. In 2D exchange NMR a given ensemble of deuteron spins after a first pulse P_1 (cf. Figure 1a) evolve with a frequency ω_e reflecting the molecular orientation at that time. Instead of generating a NMR spectrum by FT with respect to the evolution time t_1, the state of the spin system is stored by a second rf pulse P_2 and is read out again after the mixing time t_m by a third pulse P_3, which starts the detection period t_2.[14] If the molecular orientation has changed during t_m due to slow molecular reorientation, the deuteron spins now evolve with another frequency ω_d corresponding to the new molecular orientation. Note that t_m typically is substantially longer than t_1 or t_2. By repeating the experiment with an incremented value of t_1, one can generate a two-dimensional data set, which after two subsequent FTs yields a 2D exchange NMR spectrum.[18] In the

absence of motion, the frequencies ω_e and ω_d of a given ^2H spin in the evolution and detection period, respectively, are the same, and a signal along the diagonal of the spectrum is observed. In the *presence* of molecular reorientation on the time scale of t_m, the molecules can change their orientation during t_m, and the NMR frequencies ω_e and ω_d will be different. This exchange leads to off-diagonal cross peaks in the 2D spectrum (cf. Figure 1b). It demonstrates the gedankenexperiment that all C–^{2}H bonds have a single orientation corresponding to the frequency ω_e during t_1 and are changing by a jump through the angle Θ to another orientation connected with the frequency ω_d during t_2. On the two axes of the 2D spectrum the NMR spectra corresponding to the two molecular orientations before and after the mixing time, as shown in Figure 1a, are plotted. The reorientation leads to an exchange peak at the position $\omega_1 = \omega_e$ and $\omega_2 = \omega_d$. The second peak $(-\omega_e, -\omega_d)$ arises from the second transition of the spin $I = 1$ system. In reality there is an equal probability for the jump forward and backward, so that both frequencies occur in both, t_1 and t_2. This is reflected in the symmetry of the spectrum with respect to the main diagonal. The second transition of the spin $I = 1$ system leads to the mirror symmetry about the anti diagonal, so that the 2D exchange spectrum shows C_{2v} symmetry; cf. Figure 1c. From the frequency coordinates of the exchange peaks the orientation before and after the mixing time can easily be calculated with the help of eq 1. For an isotropic powder sample the exchange spectrum is not a single peak but a broad inhomogeneous pattern covering partially or even fully the 2D plane. If all molecules rotate about the same well-defined angle such that the C–^{2}H bond directions change by the angle Θ, the 2D exchange spectrum displays characteristic ridges in the form of ellipses,[9] given by the following parametric representation:

$$\omega_1 = {}^1/_2\delta(1 + 3\cos 2\vartheta)$$
$$\omega_2 = {}^1/_2\delta(1 + 3\cos(2\vartheta \pm 2\Theta)) \quad (2)$$

where ϑ serves as a parameter. Thus the so-called reorientational angle Θ is directly projected into the 2D spectrum and can be calculated from

$$|\tan\Theta| = b/a \quad (3)$$

where a and b are the principal axes of the ellipse, parallel and perpendicular to the diagonal of the spectrum. With the help of eq 3 it is possible to read off the reorientational angle Θ directly with a ruler; cf. Figure 1d. Consequently there is no model involved in obtaining this geometric information about the motional mechanism.

2D Spectra for Different Motions. It is important to realize that in general the reorientational angle Θ is not identical with the rotational angle of a polymer segment about a carbon–carbon bond or an average chain axis etc. Instead, it measures the relative angle between C–^{2}H bonds (or C_3 axes of methyl groups) before and after the rotation. The different angles are, of course, interrelated through the geometry of the chain. When only a few reorientational angles are involved in a motional mechanism, the corresponding number of ellipses is observed in the 2D exchange spectra. More complex motions will lead to a distribution of reorientational angles. The exchange spectra of diffusive motions can thus be understood as superpositions of the spectra for an infinite number of reorientational angles. Consequently, when exchange is due to diffusive motion, no sharp contours appear in the 2D exchange spectrum, but a new characteristic line shape is observed. In this way in 2D exchange spectra different motional mechanisms can be discriminated, in particular molecular reorientation by jumps and by angular diffusion.

As an illustrative example let us consider two models often employed when simulating polymer dynamics: chain motion in a diamond lattice, and chain motion by isotropic rotational diffusion. These two models, in fact, correspond to considerably different views of the molecular dynamics. Motion in a diamond lattice considers highly localized conformational transitions with fixed constraints[19–22] and involves rotations by a fixed angle $\Theta = 109.4°$, the tetrahedral angle. On the other hand, rotational diffusion of a chain in the bulk can only be visualized as a cooperative process since it involves rotation by arbitrarily small angles. Relatively broad angular distributions can, however, also occur if Brownian motion and conformational transitions with flexible constraints are considered.[23,24]

The simulated 2D exchange spectra for the two models in the limit $t_m \gg \tau_c$, where τ_c is the correlation time of the respective process, are plotted in Figure 2. The spectra are an equally weighted superposition of line shapes covering the full spectral width, corresponding to the three chain deuterons of PP, and line shapes reduced in width by a factor of 3, corresponding to the three methyl deuterons; see below.

The ellipses due to the tetrahedral jump motion on the lattice (Figure 2a) can clearly be distinguished from the broad unstructured exchange signal reflecting the broad angular distribution due to rotational diffusion (Figure 2b). The insets of Figure 2 show the even part of the reorientational angle distribution, i.e., the distribution of reorientational angles contracted to the interval $[0, \pi/2]$ since Θ and $\pi-\Theta$ cannot be distinguished for second-rank tensor interactions. This one-dimensional distribution with respect to the reorientational angle Θ is the maximum angular information one can obtain out of a single 2D exchange spectrum of powder samples in the case of axial symmetric coupling.

Experimental Section

Uniformly deuterated atactic poly(propylene) (aPP) was obtained by contacting protonated, isotactic poly(propylene) with a hydrogenation catalyst under 15 bar of deuterium at 523 K for 20 days, following the procedure of ref 25. Deuteration was effected by replacing daily the deuterium atmosphere over the sample with fresh deuterium of 99.5% isotopic purity (Matheson).[26] After isolation of the product polymer from the catalyst residue by extraction with boiling ether, purification by repeated precipitation in methanol, and redissolution in ether, the degree of deuteration and its uniformity were determined by 300-MHz ^{1}H NMR with an internal naphthalene standard. It was found that the chains were uniformly deuterated to 88%. Tacticity was assessed by 75-MHz ^{13}C NMR in *o*-dichlorobenzene at 423 K; pentad analysis revealed a diad distribution indistinguishable from a Bernoullian one with (m) = 0.48. The molecular weight by viscometry was $M_v \approx 25\,000$ (taking the Mark–Houwink constants for protonated aPP in benzene at 303 K).[27] SEC in THF indicated a molecular weight distribution similar to a most probable one. The glass transition was determined by DSC to occur at 253 K. Neutron diffraction has shown this type of sample to be completely amorphous.[27]

2D exchange spectra were taken in the temperature range from 275 to 258 K in order to obtain information about the chain dynamics in the vicinity of the glass transition. Isotactic poly(propylene) (iPP) was custom synthesized by Cambridge Isotope Laboratories, Woburn, MA, and is deuterated selectively in the methyl groups to ca. 98% as revealed by mass spectroscopy. The number-average molecular weight M_n, as determined by GPC, is 103 000, and the weight-average molecular weight M_w is 401 000, resulting in a polydispersity value of 3.98. The purification and crystallization were carried out by using

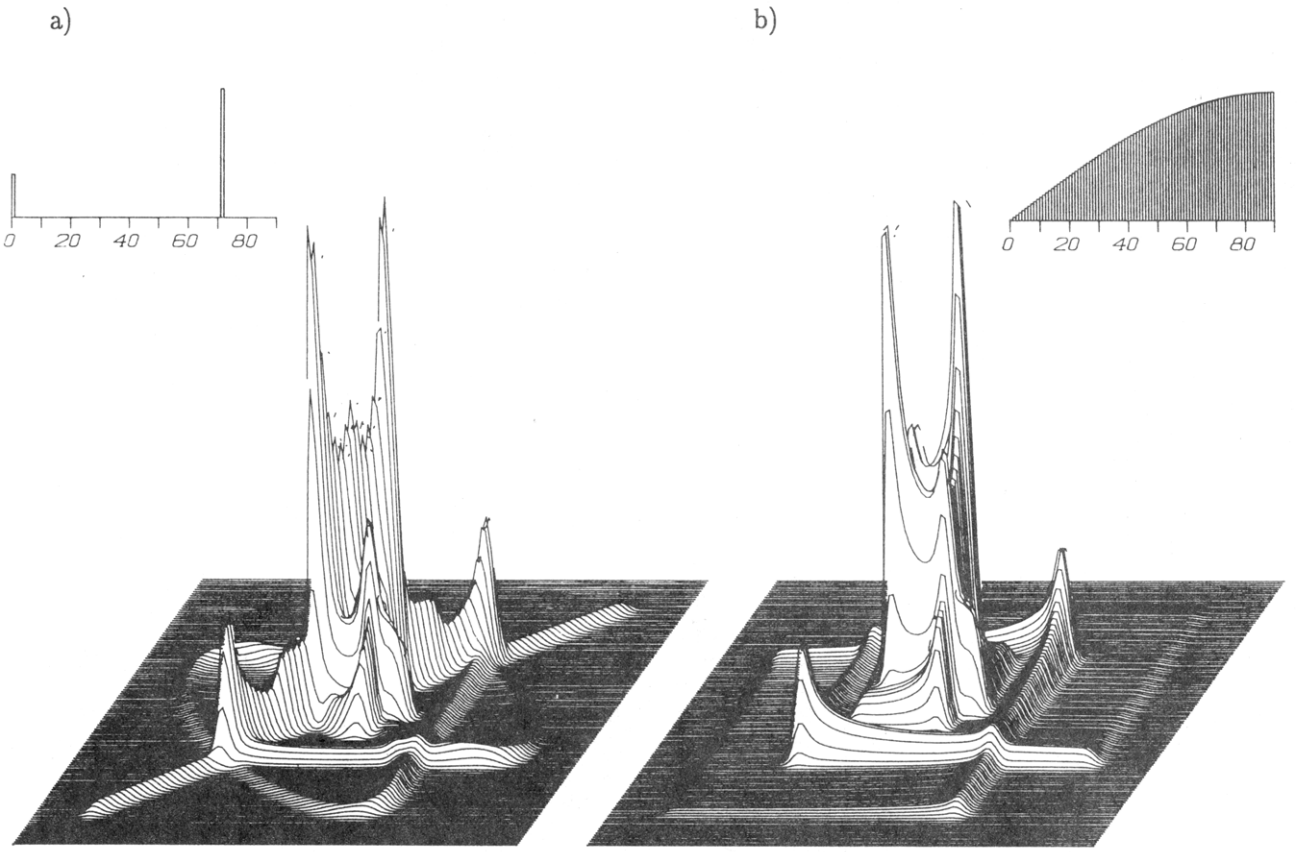

Figure 2. Simulated 2D exchange spectra for different motions in PP in the limit $t_m \gg \tau_c$. (a) 2D spectrum for chain motion in a diamond lattice showing elliptical ridges corresponding to the reorientational angle of 71.6° equivalent to the reorientational angle 180° – 71.6° = 109.4°. (b) Chain motion by isotropic rotational diffusion. The insets show the corresponding reorientational angle distributions.

solvent precipitation. iPP is a stereoregular vinyl polymer that normally develops significant crystallinity below 470 K and exists in three different modifications.[29-36] The thermodynamic most stable form (α-modification) studied in this work consists of iPP chains in the 3_1-helical conformation (...tgtgtg...) packed in a monoclinic unit cell, left- and right-handed helices being paired, with two pairs per unit cell.

The 2D exchange experiment was performed at temperatures above 360 K where in dynamic mechanical measurements the α-relaxation is observed.[1,37-43]

All NMR experiments were carried out on bulk powder samples and were performed on a Bruker CXP 300 spectrometer operating at a ^2H resonance frequency of 46.066 MHz. The duration of a 90° pulse was 3–4 μs. By applying the two four-pulse sequences that are described in detail in ref 14, two data sets were recorded to yield a pure absorption-mode 2D spectrum employing the method of ref 44. The size of the complex time-domain matrices was 50 × 128 in the case of aPP and 40 × 128 for iPP. The dimension was increased to 128 × 128 by zero filling during Fourier transformation after proper Gaussian apodization. The repetition time was set to a value of 3–5 times the longest T_1 of the sample in order to obtain fully relaxed spectra. The temperature was controlled by a Bruker VT 100 temperature unit, and the accuracy and stability in temperature were found to be ±2 K.

Results and Discussion

Glass Transition in Atactic Poly(propylene). Figure 3a shows the 2D exchange spectrum of fully deuterated atactic poly(propylene) (aPP) at a temperature of 270 K, well above the glass transition temperature T_g of 253 K. The mixing time t_m was 50 ms. Due to the presence of alkyl and methyl deuterons, the corresponding 1D spectrum consists of two Pake patterns. The outer singularities are part of the broad spectrum originating from the chain deuterons; the spectrum in the center of the 2D plane is the motionally narrowed spectrum of the methyl groups. The width of this spectrum is reduced by a factor of one-third, resulting from the rapid rotation of the methyl groups.

Elliptical ridges caused by discrete jump motions around well-defined angles are *not* visible in the spectrum. The line shape clearly points out that the motional process leads to a distribution of reorientational angles. The broadening of the Pake pattern along the main diagonal points to reorientational motion around small angles and consequently to diffusive behavior of part of the chains. The ridges parallel to the frequency axes forming the prominent square ridge and the spectral intensity covering the whole 2D plane reflect the large-angle reorientation of other chain segments. The fact that the exchange signals are spread out over the whole frequency range means that a particular C–^2H bond has a finite probability to be found in any orientation with respect to the magnetic field after the mixing time regardless of its starting position before the mixing time. This is confirmed when the reorientational angle distribution is determined from the fitted 2D spectrum as displayed in Figure 3b (see below). As mentioned previously, such a 2D exchange spectrum is identical with a two-time distribution function and consequently is an image of the state of the motional process for a fixed mixing time. Therefore a single 2D spectrum does *not* allow the determination of the specific motional mechanism. Such a conclusion, however, can be drawn out of a set of spectra with different mixing times monitoring the dynamic evolution of the system. Therefore we show in Figure 4 the development of the

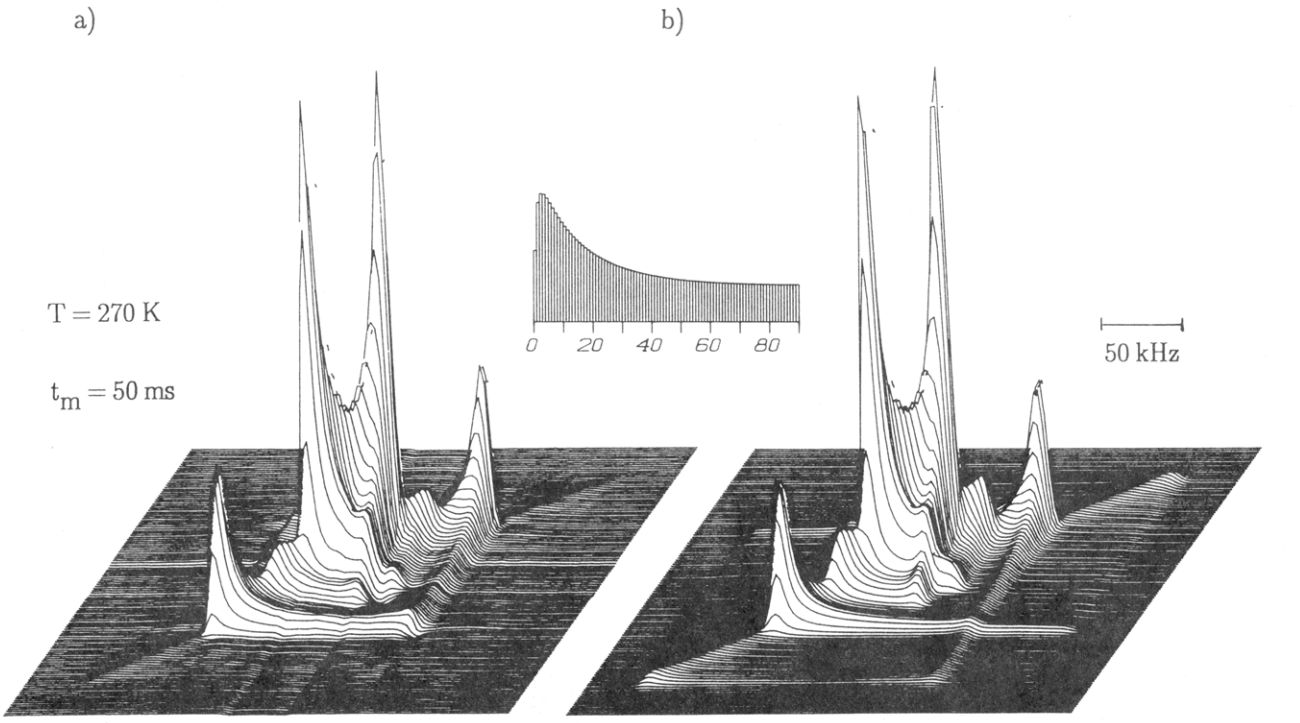

Figure 3. 2D exchange spectrum of aPP (T_g = 253 K). (a) Experiment at T = 270 K with a mixing time of t_m = 50 ms. (b) Simulation on the basis of isotropic rotational diffusion assuming a log-Gaussian distribution of correlation times, the width of which is 3 decades centered around the mean correlation time of 55 ms. The inset shows the corresponding reorientational angle distribution.

2D spectra at this temperature as a function of t_m in the range 5–200 ms.

The simultaneous observation of small- and large-angle reorientation *may* be interpreted as the result of a heterogeneous motion of the C–^{2}H bonds. Indeed, the experimental spectra for all t_m at this temperature can be described approximately by a model that assumes isotropic rotational diffusion with a log-Gaussian distribution of correlation times.[24] The full width at half-height of the distribution is 3 decades centered around the mean value of 55 ms. As an example, the simulated spectrum corresponding to the experimental spectrum in Figure 3a is shown in Figure 3b. The calculated 2D line shape was generated by a superposition of the line shapes for the different correlation times weighted with the distribution function. Further details and simulated line shapes for different widths of the distribution of correlation times are given in ref 45. In Figure 4 only the reorientational angle distributions resulting from the simulation are presented and allow for following the dynamic evolution of the system.

Our interpretation of the chain dynamics exclusively assumes small-angle reorientations as elementary steps of the motion. The final positions of the C–^{2}H bonds after the mixing time are reached as a result of numerous single steps. Of course, there *may* exist other models including large-angle fluctuations, i.e., conformational changes that are in accord with the experimental results. Indeed it is possible to simulate single spectra out of a series with varying mixing time assuming a model that combines large- and small-angle reorientation.[24] The total set of spectra, however, *cannot* be reproduced by this diffusion jump model without changing the ratio of the correlation times of the jump and the diffusive process. If these large-angle jumps are well defined, the jump process must be "slow" compared with the diffusion and/or the populations must be far from being uniform, because we do not observe any sign of elliptical ridges. Alternatively, the latter fact can be interpreted in terms of ill-defined large-angle fluctuations, which may be coupled to ill-defined angular displacements of the local environment of the mobile chain units.

When T_g is approached from higher temperatures, the slowing down of the chain dynamics is clearly visible in the 2D spectra. As an example Figure 5a shows the 2D spectrum taken at T = 264 K, thus only 6 K lower in temperature with a mixing time of 300 ms. Two points have to be mentioned in comparing this spectrum with the spectrum Figure 3a. First, the narrow spectrum clearly visible in the center of the 2D spectrum of Figure 3a is almost absent in the spectrum Figure 5a. This fact is due to the differences in the spin–lattice relaxation times[9,14] for the methyl and the chain deuterons, so that during the long mixing time the polarization of the methyl deuterons relaxes almost completely. The effect is also evident in the spectra of Figure 4 as a progressive disappearance of the narrow component with increasing mixing time. Second, the simulation yields essentially the same reorientational angle distribution, but with a mixing time being 6 times longer as in the case of the spectrum Figure 3a. This indicates the slowing down of the motional process by the same factor of 6 due to a temperature variation of only 6 K. Since the reorientational angle distribution completely determines the 2D spectrum, the broad spectrum in Figure 3a and the spectrum in Figure 5a are identical apart from the differences in intensity. Of course, this also holds for the comparison of the narrow spectrum Figure 3a with the spectrum Figure 5a but is not as obvious by reason of the difference in intensity and spectral width.

Figure 5b shows a 2D spectrum taken another 6 K closer to T_g with the same mixing time as in the case of the spectrum Figure 5a. The intensity of the exchange signal is much less at the lower temperature, showing the further slowing down of the chain dynamics. The concentration of signal intensity in the center of the main diagonal indicates that a considerable amount of C–^{2}H bonds has the same orientation before and after the mix-

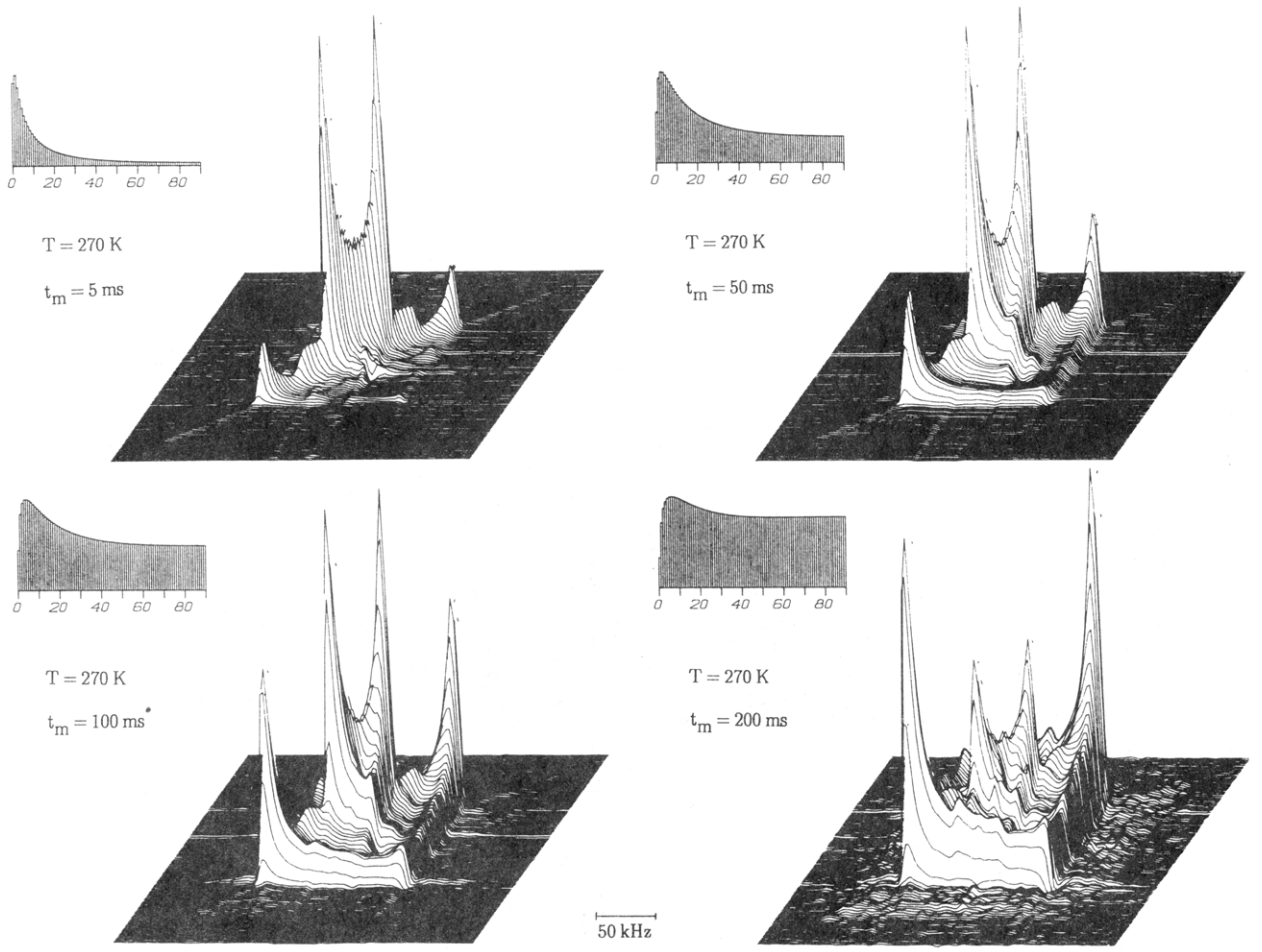

Figure 4. 2D exchange spectra of aPP (T_g = 253 K) at T = 270 K with varying mixing time t_m. The evolution of the dynamic process can be followed by inspection of the spectra or the reorientational angle distributions resulting from the simulation; cf. Figure 3.

ing time, i.e., is fixed on the time scale of the experiment. The spectra show that close to T_g the 2D exchange experiment is able to detect rotations of individual chain segments through a few degrees on the time scale of seconds. Thus, the ultraslow processes connected with the glass transition can be monitored on a molecular level. When the virtual activation energy of the motion is determined from an Arrhenius plot covering a range of mean correlation times from 4 ms at 275 K to 12 s at 258 K, based on a total number of 15 2D spectra, a value of (274 ± 50) kJ/mol results. This is unphysically high for a segment motion and points to collective dynamic behavior. In fact, the temperature variation of the average correlation times τ of the motional process follows the Williams–Landel–Ferry (WLF) equation[46]

$$\log \frac{\tau(T)}{\tau(T_g)} = -\frac{C_1(T - T_g)}{C_2 + T - T_g} \tag{4}$$

where C_1 and C_2 are constants. The WLF equation is interpreted as an intrinsic dependence of the rate of irreversible processes on the fractional volume available[47] and is equivalent to the explicit free volume Doolittle equation.[48] When our data are combined with the ^{13}C spin–lattice relaxation measurements of Mandelkern et al.[49] at temperatures above 300 K, the mean correlation times cover a dynamic range of 11 decades of magnitude. As shown in Figure 6 they are quantitatively fitted by a WLF curve with C_1 = 18.2 and C_2 = 47.6 K. The correlation time at T_g was extrapolated to be 1000 s. Similar values for C_1 and C_2 can be calculated from refs 50 and 51, where the Vogel–Fulcher–Tamman–Hesse (VFTH) equation, which is an alternative form of the WLF equation, has been applied to photon correlation spectroscopy and shear creep measurement results.

The fact that our data agree with the WLF equation indicates that the local dynamics monitored by 2D NMR is intimately linked to the collective dynamics of the glass process. Like results have been obtained in ref 45, where the 2D exchange experiment has been employed to study the chain dynamics of atactic poly(styrene) in the vicinity of the glass transition. This nicely corroborates our statement that rotational diffusion of polymer chains can only be visualized as a cooperative process.

Helical Jumps in Isotactic Poly(propylene). In contrast to the chain motion at the glass transition the rotation of the stereoregular iPP chains in the crystalline regions occurs through well-defined angles. Figure 7 shows the 2D exchange spectrum of methyl-deuterated iPP taken at T = 387 K with a mixing time of 150 ms. As mentioned previously, the rapid rotation of the methyl group results in an averaged field gradient tensor along the C_3 axis which serves to probe the dynamics of the main chain. On the diagonal of the spectrum the conventional 1D deuteron NMR spectrum appears. The broad signals originate from the crystalline regions of the partially crystalline polymer, the narrow signal in the center of the spectrum from the mobile amorphous regions. The off-diagonal exchange signal exhibits sharp ridges in the form of ellipses, indicative of discrete jump motion around a well-defined angle. To enhance the visibility of these ridges the narrow signal is cut off in the plot to the same height as the singularities of the broad spectrum. Figure 8a gives

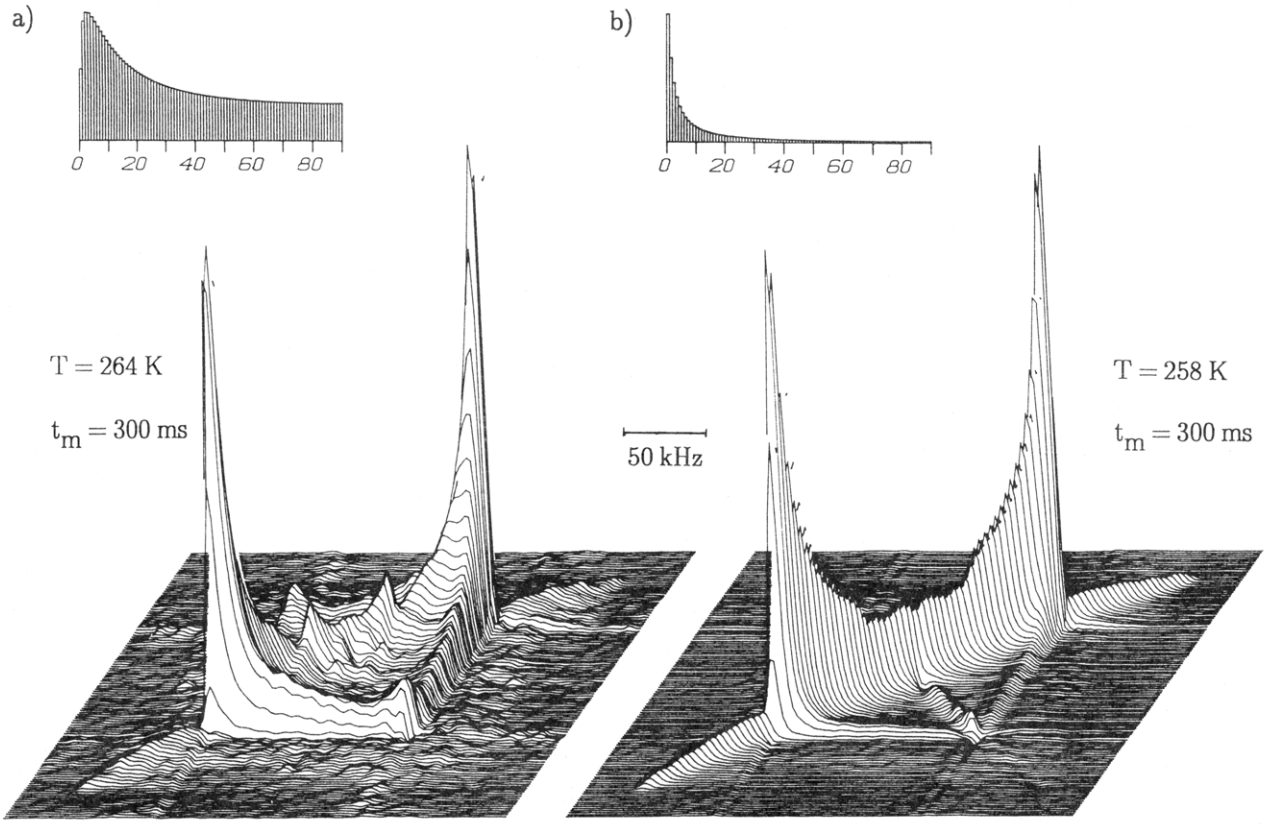

Figure 5. 2D exchange spectra of aPP (T_g = 253 K). (a) Experimental spectrum at T = 264 K with a mixing time of t_m = 300 ms. (b) Experimental spectrum at T = 258 K with t_m = 300 ms. The slowing down of the motional process is clearly visible from the spectra or the reorientational angle distributions.

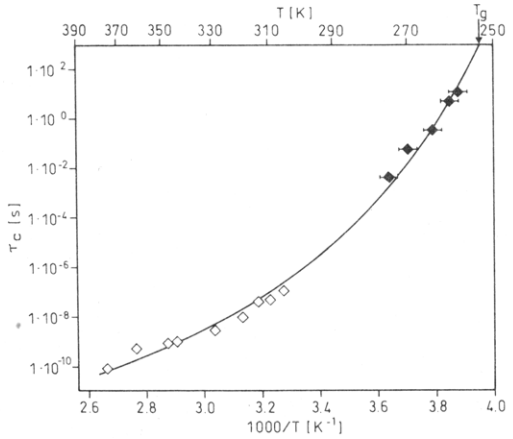

Figure 6. WLF fit of the mean correlation times resulting from the simulation of the aPP spectra. Filled squares, 2D exchange NMR; open squares, ^{13}C spin–lattice relaxation measurements (Mandelkern et al.[49]).

a ridge plot of the spectrum Figure 7, displaying only the local maxima of the 2D spectrum. The two ellipses arising from the two transitions of a spin I = 1 system are clearly discernible. From the shape of the ellipses, the reorientational angle can be determined model free as described above, yielding a value of 113°. The error of the determination of this value is estimated to be ±2°. The slight broadening of the ellipses in the region of the main diagonal indicates that besides this value, reorientational angles between 111° and 115° are involved in the motion, the maximum of this distribution being given by 113°. Figure 8b gives a ridge plot for these three different reorientational angles, where the widest ellipse corresponds to the largest angle and the narrowest ellipse to the smallest reorientational angle.

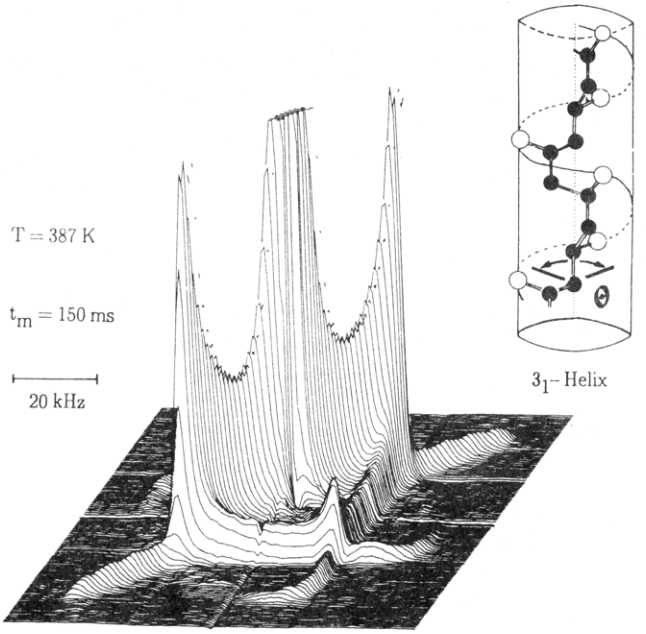

Figure 7. 2D exchange spectrum of iPP. Experimental spectrum at T = 387 K with a mixing time t_m = 150 ms. The inset shows the 3_1 helix of iPP. The elliptical ridges in the 2D plane correspond to a reorientational angle of 113°. This value results from discrete jumps in 120° steps about the helix axis.

An indication of the molecular origin of the jump process is given by considering the structure of iPP. In the crystalline domains iPP forms a 3_1 Helix, for convenience of the reader given in Figure 7. The symmetry of the helix allows a rotational jump motion of the polymer chain about the helix axis, presumably in connection with a translation. Consequently a given monomer unit after the jump occupies the position of the neigh-

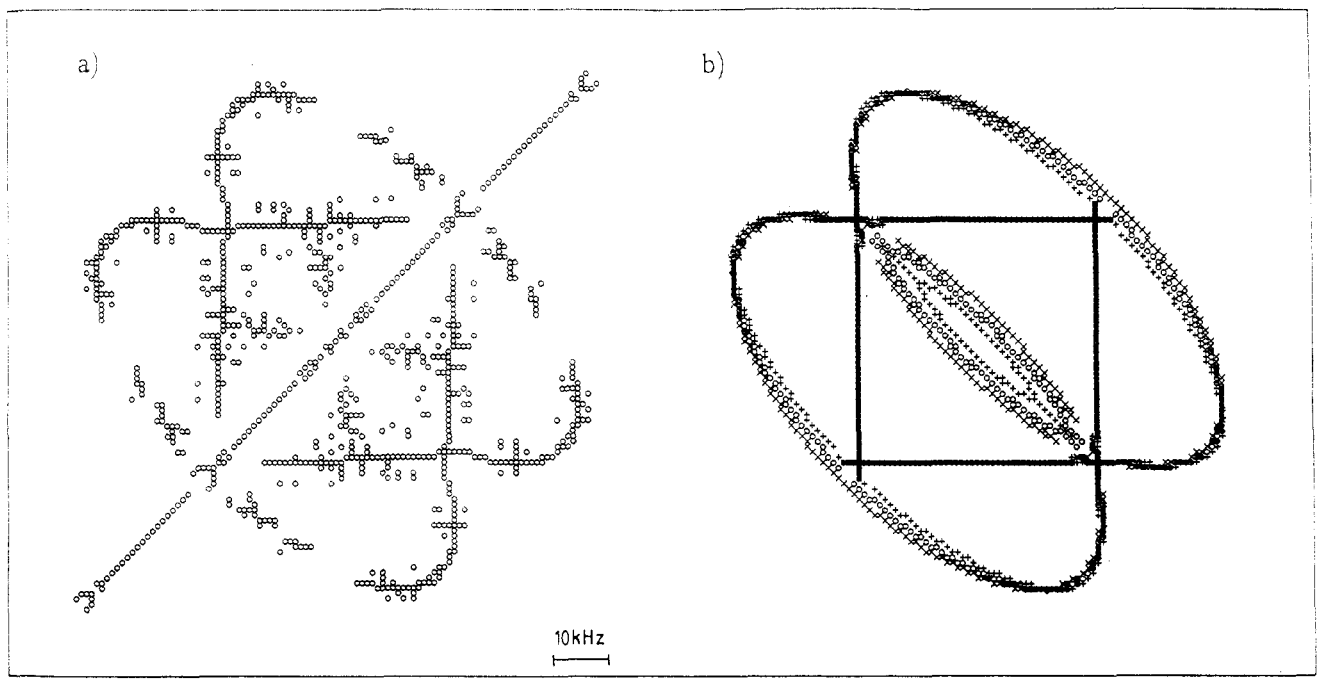

Figure 8. (a) Ridge plot of the iPP spectrum Figure 7. The two ellipses correspond to the two transitions of the spin $I = 1$ system. (b) Ridge plot of the calculated ellipses for the reorientational angles of 111° (+), 113° (○), and 115° (×).

boring monomer unit before the jump. This reorientational angle between the methyl groups is consistent with a rotational jump motion of the helix in discrete steps of 120° about the helix axis. In addition, the observed reorientational angle is in agreement with the value calculated from the crystallographic data of ref 33, yielding a value of ca. 111°. The observation of helical jumps is corroborated by ^{13}C 2D exchange spectroscopy where exchange signals for all three carbons having different chemical shifts are observed.[52] All 2D experiments were performed in a temperature region where in dynamic mechanic and dielectric measurements the "α-relaxation" is observed. Most investigators, although differing in their detailed interpretation, have concluded that the α-relaxation arises from the crystalline regions of the polymer.[1,37-43] The activation energy ranges from 48 to 70 kcal/mol, and the mechanism is assumed to consist of a single process only. Kawai et al.[53] recently suggested that the α-process is an intralamellar phenomenon that involves intracrystalline chain motions and lamellar reorientation such as tilting or detwisting. Unfortunately, the short spin–lattice relaxation time of the rapidly rotating methyl group prevents us from following the helical jump motion down to lower temperatures and determining its activation energy. In poly(oxymethylene) (POM), another semicrystalline polymer with helical conformation, 2D ^{13}C experiments on static as well as rotating samples have established a similar helical jump motion in the crystalline regions and its relation to the mechanical α-relaxation.[52] We therefore conclude that the helical jumps in iPP likewise are responsible for the α-relaxation.

Concluding Remarks

This 2D NMR study of the chain motion in poly(propylene) of different conformation and packing shows that the differences between crystalline and amorphous states are directly reflected in the motional behavior: the chain motion in crystalline polymers involves a limited number of reorientational angles consistent with the crystal structure, in the case of iPP helical jumps. The chain motion of aPP at the glass transition involves a broad distribution of reorientational angles, reflecting the amorphous nature of the glassy state. In both cases, however, the motional processes detected this way are directly related to the mechanical behavior.

Acknowledgment. We thank Dr. S. Kaufmann and K. Schmidt-Rohr for numerous valuable discussions concerning the data analysis. Financial support of the Deutsche Forschungsgemeinschaft, SFB 262, is gratefully acknowledged.

References and Notes

(1) McCrum, N. G.; Read, B. E.; Williams, G. *Anelastic and Dielectric Effects in Polymeric Solids*; Wiley: New York, 1967.
(2) Ferry, J. D. *Viscoelastic Properties of Polymers*; Wiley: New York, 1980.
(3) Bailey, R. T.; North, A. M.; Pethrick, R. A. *Molecular Motion in High Polymers*; Clarendon Press: Oxford, 1981.
(4) Hedvig, P. *Dielectric Spectroscopy of Polymers*; Adam Hilger: Bristol, 1977.
(5) Spiess, H. W. In *Adv. Polym. Sci.* **1985**, *66*, 23.
(6) Spiess, H. W. *Colloid Polym. Sci.* **1983**, *261*, 193.
(7) Voelkel, R. *Angew. Chem., Int. Ed. Engl.* **1988**, *27*, 1468.
(8) Jelinski, L. W. *High Resolution NMR Spectroscopy of Synthetic Polymers in Bulk*; Komoroski, R. A., Ed.; VCH Publishers: Deerfield Beach, FL, 1986.
(9) Schmidt, C.; Wefing, S.; Blümich, B.; Spiess, H. W. *Chem. Phys. Lett.* **1986**, *130*, 84.
(10) Hagemeyer, A.; Brombacher, L.; Schmidt-Rohr, K.; Spiess, H. W. *Phys. Rev. Lett.*, submitted.
(11) Wefing, S.; Spiess, H. W. *J. Chem. Phys.* **1988**, *89*, 1219.
(12) Spiess, H. W. *J. Chem. Phys.* **1980**, *72*, 6755.
(13) Blümich, B.; Spiess, H. W. *Angew. Chem.* **1988**, *100*, 1716; *Angew. Chem., Int. Ed. Engl.* **1988**, *27*, 1655.
(14) Schmidt, C.; Blümich, B.; Spiess, H. W. *J. Magn. Reson.* **1988**, *79*, 269.
(15) Abragam, A. *The Principles of Nuclear Magnetism*; Oxford University Press: Oxford, 1961.
(16) Spiess, H. W. In *NMR—Basic Principles and Progress*; Diehl, P., Fluck, E., Kosfeld, R., Eds.; Springer-Verlag: Berlin, 1978; Vol. 15.
(17) Pake, G. E. *J. Chem. Phys.* **1948**, *16*, 327.
(18) Ernst, R. R.; Bodenhausen, G.; Wokaun, A. *Principles of Nuclear Resonance in One and Two Dimensions*; Clarendon Press: Oxford, 1987.
(19) Rosenke, K.; Sillescu, H.; Spiess, H. W. *Polymer* **1980**, *21*, 757.
(20) Gény, F.; Monnerie, L. J. *J. Polym. Sci., Polym. Phys. Ed.* **1979**, *17*, 131, 147.

(21) Rosenke, K.; Zachmann, H. G. *Prog. Colloid Polym. Sci.* **1978**, *64*, 245.
(22) Schmeddig, P.; Zachmann, H. G. *Kolloid Z. Z. Polym.* **1972**, *250*, 1105.
(23) Helfand, E.; Wassermann, Z. R.; Weber, T. B.; Skolnick, J.; Runnels, J. R.; *J. Chem. Phys.* **1971**, *75*, 4441.
(24) Wefing, S.; Kaufmann, S.; Spiess, H. W. *J. Chem. Phys.* **1988**, *89*, 1234.
(25) Suter, U. W.; Neuenschwander, P. *Macromolecules* **1981**, *14*, 528.
(26) Theodorou, D. N. Ph.D. Thesis, MIT, 1985.
(27) Dannsso, F.; Moraglio, G. *Makromol. Chem.* **1958**, *28*, 250.
(28) Theodorou, D. N.; Ludovice, P. J.; Suter, U. W. In *Scattering, Deformation and Fracture in Polymers*; Wignall, G. D., Crist, B., Russell, T. P., Thomas, E. L., Eds.; *Material Research Society Symposia Proceedings* **1986**, *79*, 387.
(29) Samuels, R. J. *Structured Polymer Properties*; Wiley: New York, 1974.
(30) Natta, G. *Makromol. Chem.* **1960**, *35*, 94.
(31) Turner-Jones, A.; Aizlewood, J. M.; Beckett, D. R. *Makromol. Chem.* **1964**, *75*, 134.
(32) Addink, E. J.; Beintema, J. *J. Polym. Sci.* **1961**, *2*, 185.
(33) Mencik, Z. *J. Macromol. Sci.—Phys.* **1972**, *B6* (1), 101.
(34) Bunn, A.; Cudby, M. E. A.; Harris, R. K.; Packer, K. J.; Say, B. J. *Polymer* **1982**, *23*, 694.
(35) Gomez, M. A.; Tanaka, H.; Tonelli, A. E. *Polymer* **1987**, *28*, 2227.
(36) Wright, N. F.; Taylor, P. L. *Polymer* **1987**, *28*, 2004.
(37) Flocke, H. A. *Kolloid-Z.* **1962**, *180*, 118.
(38) McCrum, N. G. *Makromol. Chem.* **1959**, *34*, 50.
(39) Sauer, J. A.; Wall, R. A.; Fuschillo, N.; Woodward, A. E. *J. Appl. Phys.* **1958**, *29*, 1385.
(40) Krämer, H.; Helf, K.-E. *Kolloid-Z.* **1962**, *180*, 114.
(41) McBrierty, V. J.; Douglass, D. C.; Falcone, D. R. *J. Chem. Soc., Faraday Trans. 2* **1972**, *68*, 1051.
(42) Roy, S. K.; Kyu, T.; St. John Manley, R. *Macromolecules* **1988**, *21*, 499.
(43) McCall, D. W. *Natl. Bur. Stand. U.S. Spec. Publ.* **1969**, *301*, 475.
(44) States, D. J.; Haberkorn, R. A.; Ruben, D. J. *J. Magn. Reson.* **1982**, *48*, 286.
(45) Kaufmann, S.; Wefing, S.; Schaefer, D.; Spiess, H. W. *J. Chem. Phys.*, submitted.
(46) Williams, M. L.; Landel, R. F.; Ferry, J. D. *J. Am. Chem. Soc.* **1955**, *77*, 3701.
(47) Haward, R. N. *The Physics of Glassy Polymers*; Applied Science Publishers: London, 1973.
(48) Doolittle, A. K. *J. Appl. Phys.* **1951**, *22*, 1471; **1952**, *23*, 236.
(49) Dekmezian, A.; Axelson, D. E.; Dechter, J. J.; Borah, B.; Mandelkern, L. *J. Polym. Sci., Polym. Phys. Ed.* **1985**, *23* (2), 367.
(50) Fytas, G.; Ngai, K. L. *Macromolecules* **1988**, *21*, 804.
(51) Plazek, D. L.; Plazek, D. J. *Macromolecules* **1983**, *16*, 1469.
(52) Hagemeyer, A.; Schmidt-Rohr, K.; Spiess, H. W. *Adv. Magn. Reson.* **1989**, *13*, 85.
(53) Kawai, H.; Hashimoto, T.; Suehiro, S.; Fujita, K. *Polym. Eng. Sci.* **1984**, *24*, 361.

Synthesis and Characterization of New Polymers Exhibiting Large Optical Nonlinearities. 1. Ladder Polymers from 3,6-Disubstituted 2,5-Dichloroquinone and Tetraaminobenzene

Luping Yu and Larry R. Dalton*

Department of Chemistry, University of Southern California, Los Angeles, California 90089-0482

Received November 20, 1989; Revised Manuscript Received January 30, 1990

ABSTRACT: Ladder polymers were synthesized from 3,6-disubstituted 2,5-dichloroquinones and tetraaminobenzene. The precursor to these polymers can be dissolved in organic solvents such as DMF, DMSO, and DMA. This solubility permits convenient processing of polymers into thin films which can subsequently be converted to fully fused-ring ladder polymers by thermal treatment. the final ladder polymers exhibited exceptional thermal stability (as determined by TGA) and laser damage thresholds in excess of 1 GW/cm^2. Degenerate four-wave-mixing measurements on these ladder polymers yielded third-order susceptibilities as high as 1.6×10^{-9} esu, which is one of the highest values observed for an amorphous material.

Many organic and polymeric materials containing extended conjugated systems have been shown to exhibit large, ultrafast second- and third-order nonlinear optical susceptibilities.[1-3] A large number of potential applications, ranging from optical computing to sensor protection, exist for these materials. The most investigated polymer system is poly(diacetylene) (PDA), which has exhibited third-order susceptibilities as high as 8×10^{-10} esu for single crystals;[3] however, amorphous PDA exhibits a much smaller $\chi^{(3)}$. If practical applications of polymers to the fabrication of nonlinear optical devices are to be pursued, then new polymer materials with much higher nonlinear optical susceptibilities, higher laser damage thresholds, improved optical transparency, and improved processibility must be developed. It is the search for such materials that motivates the present work.

Theory provides the direction for the development of new polymers. It is generally recognized that third-order susceptibility increases dramatically with π-electron delocalization.[4] Ladder polymers with the structure shown in Figure 1 not only possesses a conjugated π-electron system but the forced planarity of these polymers ensures optimum electron delocalization (the effectiveness of overlap of p orbitals is determined by θ, the dihedral angle between p orbitals, through $\cos^2 \theta$). Theory predicts that even oligomers of these materials will exhibit significant third-order susceptibilities.[5] Scaling arguments would suggest significant increases in optical nonlinearity of polymers relative to the oligomeric compounds, although the increases would not be expected to continue indefinitely with polymer chain length due to self-localization effects (determined by intrinsic electron–phonon and electron–

0024-9297/90/2223-3439$02.50/0